

Visible light photocatalytic properties of nano-sized tin dioxide doped with iron.



M. Samsonenko¹, S. Khalameida¹, V. Starchevskyy², L. Kotynska¹

¹ Institute for Sorption and Problems of Endoecology, NAS of Ukraine.

E-mail: mashuna.08@gmail.com

² Institute of Chemistry and Chemical Technology, L'viv National Polytechnic University.

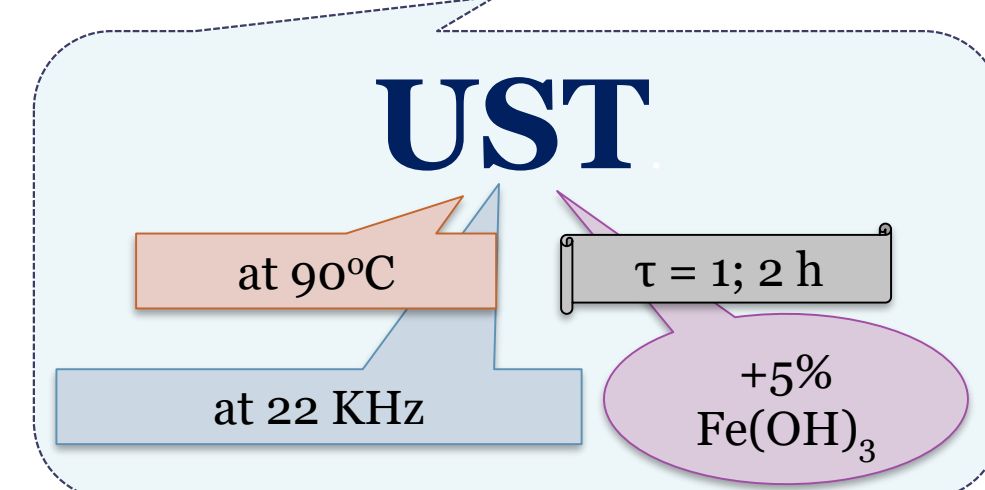
The application of nano-sized oxides for photocatalytic degradation is a promising method of wastewater treatment. The use of visible light simplifies and reduces the cost of this process. One of the promising photocatalysts is tin dioxide. To increase the efficiency of its use in photocatalytic processes under the action of visible light, can use its doping with transition metals. It is known that the use of iron as a doped additive to titanium dioxide can increase photocatalytic activity including through inhibition of electron/hole pairs recombination. For SnO₂, this approach has been little studied.

The aim of this work

Study the effect of sonochemical doping on the photocatalytic properties of iron-doped tin dioxide.

EXPERIMENTAL

The high porous gel SnO₂ heterogeneously **precipitated** using ammonia
 $\text{SnCl}_4 + 4\text{NH}_3 + \text{H}_2\text{O} \rightarrow \text{SnO}_2 + 4\text{NH}_4\text{Cl}$
 $S = 178 \text{ m}^2/\text{g}$



Thermal treatment at 300°C

Physical-chemical properties of all samples were studied using the following techniques: differential thermal analysis, X-ray analysis, nitrogen adsorption-desorption, UV-Vis spectroscopy

Photocatalytic activity
 Aqueous solution of **Rhodamine B, Safranin T, 4-chlorophenol**
 $(C = 1 \cdot 10^{-5} \text{ mol/L}; C_{\text{photocatal.}} = 1 \text{ g/L};$
 LED lamp Philips LED Cool daylight
 $\text{power} = 100 \text{ W}; \lambda_{\text{max}} = 580 \text{ nm}; \tau = 10 \text{ h}.$

RESULTS

According to the results of DTA-TG, the initial precipitated sample corresponds to the composition of tin oxhydroxide. Doping by ultrasonic treatment leads to the removal of the OH group. Next thermal treatment of the doped sample promotes this process. All obtained samples have a composition close to SnO₂.

The doped samples have a more perfect crystalline structure than the initial precipitated sample. Doping and thermal treatment of samples leads to an increase in the size of the crystallites.

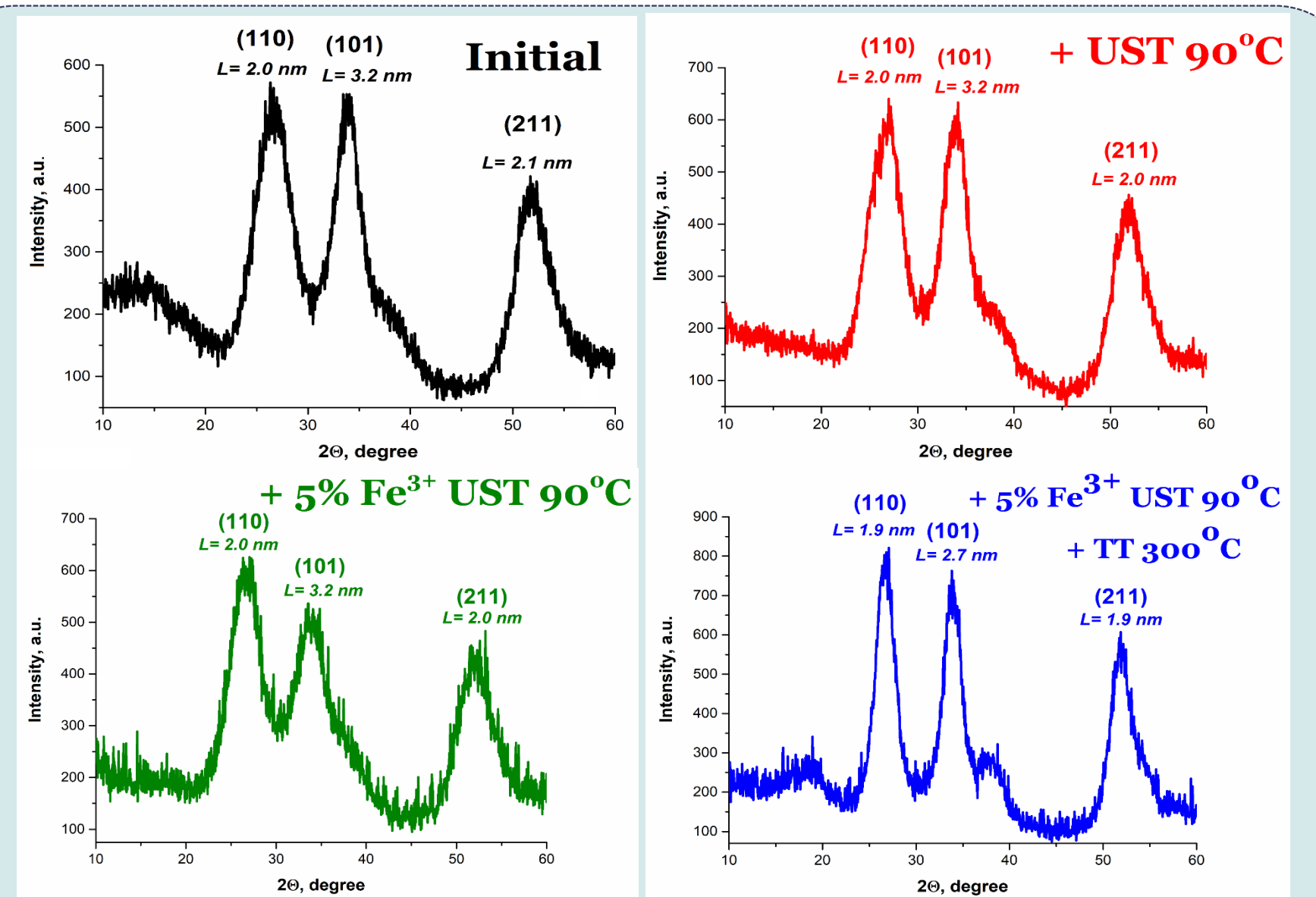


Fig. 1. Data of XRD

Table 1. Tin (IV) oxide porous structure parameters

Samples	S, m ² /g	V _Σ	cm ³ /g			d _{me} nm
			V _{ma}	V _{me}	V _{mi}	
SnO ₂ precipitated	178	0.09	0.00	0.02	0.07	2.4
+ UST 90°C	206	0.11	0.01	0.02	0.08	2.5
+5%Fe UST 90°C	205	0.25	0.14	0.03	0.08	2.5
+5%Fe UST 90°C+TT300°C	137	0.26	0.09	0.08	0.08	4.7

S - specific surface area, V_Σ - pore volume, V_{me} - mesopores volume, V_{mi} - micropores volume, V_{ma} - macropores volume, d_{me} - diameter of mesopores (calculated from the pore size distribution (PSD)).

The initial sample is microporous with high value of specific surface area. After UST, an increase in the specific surface area is observed; the total volume and pore size are almost unchanged. The doping with Fe³⁺ has a similar effect. In this case, the doped SnO₂ has porous structure with high the proportion of micropores in the total pore volume, but meso- and macropores are presented. After further thermal treatment occurs: the specific surface area decrease, and the volume and size of mesopores increases (Table). The formation of meso-macroporous structure is observed.

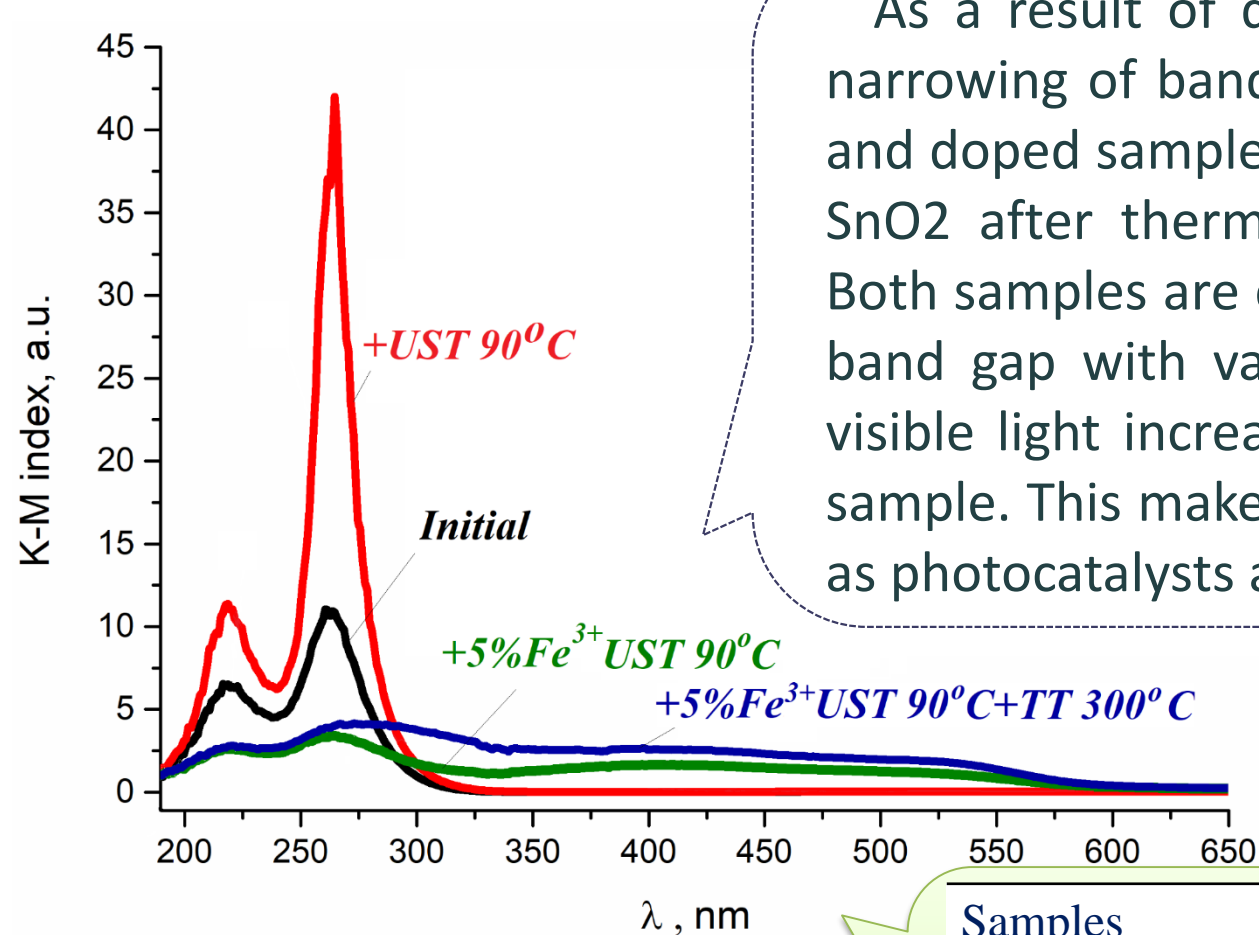


Fig. 2. Data of UV-Vis spectroscopy

As a result of doping with Fe³⁺, there are a significant narrowing of band gap E_g from 4.2 eV to 3.7 eV for initial and doped samples, respectively. The band gap E_g of doped SnO₂ after thermal treatment also decreases to 2.9 eV. Both samples are characterized by an additional sublevel in band gap with values at 2 eV. As well as, absorption of visible light increases 3-4 times compared with un-doped sample. This makes it possible to use the obtained samples as photocatalysts active under visible light.

$$E_g = 1239.5 / \lambda,$$

where λ - absorption edge, nm.

Samples	λ (nm)	E _g (eV)	A(%)
initial	295	4.2	15
+UST 90°C	288	4.3	18
+Fe ³⁺ UST 90°C	335	3.7	70
+Fe ³⁺ UST 90°C+TT300°C	427	2.9	77

λ—absorption edge, nm; E_g—band gap, eV; A—light absorption in the visible region, %.

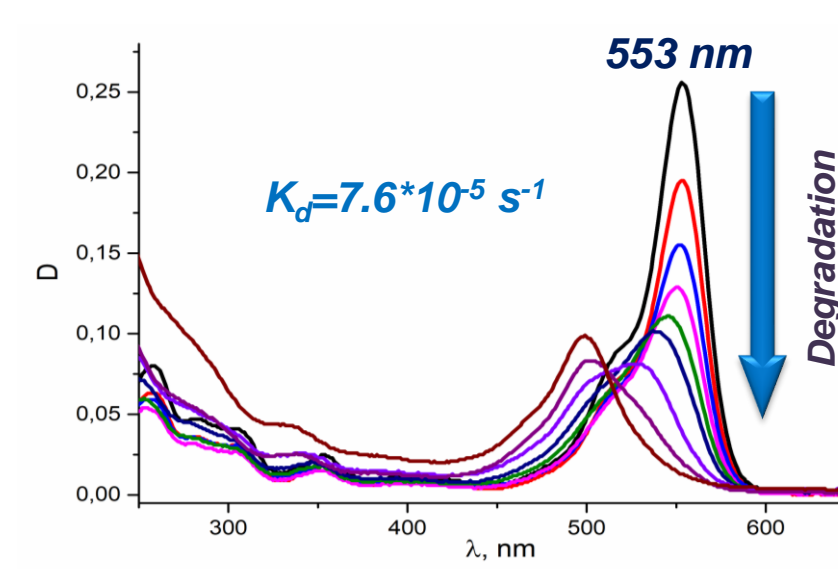


Fig. 3. UV-Vis spectra of RhB aqueous solution after its photodegradation in the presence of 5%Fe³⁺ + SnO₂ after UST at 90°C.

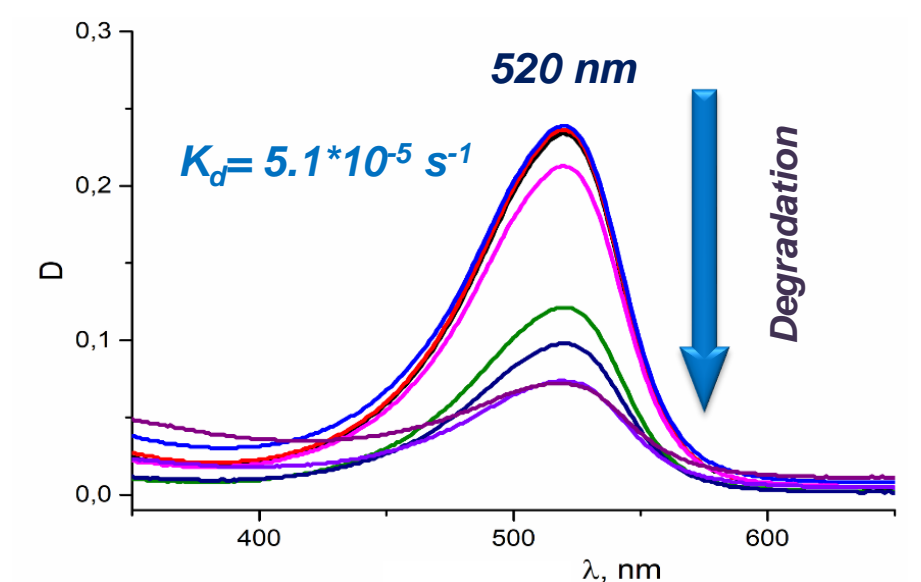


Fig. 4. UV-Vis spectra of ST aqueous solution after its photodegradation in the presence of 5%Fe³⁺ + SnO₂ after UST at 90°C.

These transformations of physico-chemical parameters contribute to the increase in photocatalytic activity of iron-doped tin dioxide in processes of the dyes degradation under visible light. The rate constant of rhodamine B and safranin T degradation for Fe-doped SnO₂ is increasing 2-3 times. In addition, in contrast to inactive initial tin dioxide, doped samples exhibit photocatalytic activity during the degradation of 4-chlorophenol under visible irradiation.

This work was supported by the framework of the research project of young scientists from the National Academy of Sciences of Ukraine «Alternative methods of doping SnO₂-based materials to purification of the water environment from pollutants», (contract no :75-09/03-2022).